



**HAL**  
open science

## Aging response investigation of 2017 Al alloy processed by gravity and squeeze casting

Najib Souissi, Catherine Mabru, Chedly Bradai

### ► To cite this version:

Najib Souissi, Catherine Mabru, Chedly Bradai. Aging response investigation of 2017 Al alloy processed by gravity and squeeze casting. *International Journal of Materials Research*, 2019, 110 (9), pp.859-864. 10.3139/146.111806 . hal-02315264

**HAL Id: hal-02315264**

**<https://hal.science/hal-02315264>**

Submitted on 14 Oct 2019

**HAL** is a multi-disciplinary open access archive for the deposit and dissemination of scientific research documents, whether they are published or not. The documents may come from teaching and research institutions in France or abroad, or from public or private research centers.

L'archive ouverte pluridisciplinaire **HAL**, est destinée au dépôt et à la diffusion de documents scientifiques de niveau recherche, publiés ou non, émanant des établissements d'enseignement et de recherche français ou étrangers, des laboratoires publics ou privés.



## Open Archive Toulouse Archive Ouverte (OATAO)

OATAO is an open access repository that collects the work of some Toulouse researchers and makes it freely available over the web where possible.

This is an author's version published in: <https://oatao.univ-toulouse.fr/24337>

**Official URL** : <http://doi.org/10.3139/146.111806>

### To cite this version :

Souissi, Najib and Mabru, Catherine and Bradai, Chedly Aging response investigation of 2017 Al alloy processed by gravity and squeeze casting. (2019) International Journal of Materials Research, 110 (9). 859-864. ISSN 1862-5282

Any correspondence concerning this service should be sent to the repository administrator:

[tech-oatao@listes-diff.inp-toulouse.fr](mailto:tech-oatao@listes-diff.inp-toulouse.fr)

# Aging response investigation of 2017 Al alloy processed by gravity and squeeze casting

Suitable pressure levels and heat treatment of casting wrought aluminum alloy are key process parameters in making components with better metallurgical properties. For this purpose, the effect of applied pressure and aging treatment on the microstructure and the mechanical properties of an industrial 2017 aluminum alloy manufactured by gravity and direct squeeze casting processes are investigated in this paper. After treating to various aging states, the correlation between these parameters and the characteristics of the cast alloy has been analyzed and discussed.

**Keywords:** Squeeze pressure; 2017 Al alloy; Aging temperature; Microstructure; Mechanical properties

## 1. Introduction

Among the different techniques described for materials forming, the squeeze casting (SC) process is used to produce high integrity and low cost aluminum alloy [1]. During the solidification of the melt, the direct action of pressure activates two principal phenomena that are not generally observed in traditional die casting methods. First, the pressure generates a high cooling rate due to the reduction of the air gap between the metal and the die wall, hence, there is a much larger effective contact area [2]. In addition to that, the temperature of the liquidus could rise upon application of pressure, leading to a higher degree of undercooling [3]. The change in the nucleation ratio and cooling rate would increase, which creates a finer grain size [3]. The second phenomenon caused by SC is the fact that direct applied pressure inhibits defects associated with shrinkage cavities and porosity formation [4]. This eliminates casting drawbacks and results in a better quality of casting products with a much higher density. On the other hand, heat treatment processing is considered as a promising method to improve the quality of aluminum alloys. Yet, some research studies investigating the effect of heat treatment process on casting wrought Al alloys have been reported in literature [5–8]. In this regard, Kim et al. [6] studied the effect of aging times on the microstructure and mechanical properties of 7075 Al alloy. The results show that the fine-grained structures and the uniform distribution of eutectics at the periphery of the grain boundaries caused significant changes in hardness and tensile strength of specimens. Skolianos et al. [7] assessed the influence of T6 heat treatment on the microstructure and tensile proper-

ties of squeeze cast 6061 Al alloy and found that the strength of the alloy decreases with the presence of the  $(\text{FeCrMn})_3\text{SiAl}_{12}$  phase and increases with that of the finely dispersed  $\text{Mg}_2\text{Si}$  phase. Zhang et al. [8] reported that the heat treatment caused an improvement of the tensile strength and elongation of SC Al–Cu based alloy. However, reports on aging temperature effect of SC wrought Al alloy are very few. It must be noted that precipitation behavior is known to have an important influence on the metallurgical properties of Al alloys.

Al-4 wt.%Cu (2xxx series) alloys are a precipitation hardening in which Cu promotes the formation of  $\theta$ - $\text{Al}_2\text{Cu}$  precipitates. The decomposition of the supersaturated solid solution (SSS) is believed to proceed in the following steps:  $\text{SSS} \rightarrow \text{Guinier–Preston (GP) zones} \rightarrow \theta'' \rightarrow \theta' \rightarrow \theta$ - $\text{Al}_2\text{Cu}$  [9]. Obviously, the development of high-performance alloys requires a great understanding of the relationship between processing parameters and mechanical properties through a quantitative prediction of the precipitation behavior. More specifically, wrought 2017 aluminum alloy, which is widely used in aircraft and aerospace structures [10, 11], has gained a growing interest in it especially when formed by the SC technique [12–15]. Moreover, it is reported that the combination of squeeze pressure and heat treatment offers several advantages that make wrought aluminum alloys acquire improved mechanical properties [6, 8]. An understanding of the interrelationships between these parameters is particularly important since the mechanical properties of casting components are highly correlated with the final microstructure and crystallographic texture. Thus, the main objective of the present work is to investigate the effects of the aging temperature and to develop a suitable age-hardening heat-treatment process for gravity die casting (GC) and SC wrought 2017 Al alloy. It focuses on the relationship between the microstructure and the mechanical behavior of the material.

## 2. Experimental procedure

### 2.1. Material and specimen preparation

The casting experiments were conducted using a 2017 Al aluminum alloy, which is widely used as wrought product in various mechanical areas [16, 17]. Its chemical composition, as determined by spectral analysis, is shown in Table 1.

It was received as an extruded bar of diameter 80 mm and melted at 700 °C in a graphite crucible using an electric resistance furnace. The casting process was carried out

Table 1. Chemical composition of 2017 A aluminum alloy.

Elements	Cu	Mg	Si	Fe	Mn	Ni	Pb	Zn	Cr	Al
Mass %	4.47	0.4	0.52	0.65	0.37	0.1	0.03	0.25	0.1	Bal.

through a solid mold and a punch made from heat treated H13 steel.

The direct SC experiments were conducted on a hydraulic press, where the pressure on the molten metal is kept at 90 MPa until the end of solidification. In GC, molten alloy was poured directly into the die without external pressure. The mold was preheated up to 200 °C. The as-cast billets were rod-shaped; 23 mm in diameter and 110 mm in length. The choice of casting parameters was based on previous works [12–14]. Afterwards, the billets were solution treated at 500 °C for 8 h followed by water quenching. In order to investigate the effects of aging temperature and the applied pressure on the microstructure and mechanical properties, some quenched specimens were placed in the furnace (6 h) for the artificial aging process at different temperatures. Figure 1 shows an overall scheme of the elaboration process and the experimental set-up followed in the present study.

## 2.2. DSC analyses

The differential scanning calorimetry (DSC) experiments were conducted on a SETARAM DSC-92 instrument for temperatures ranging from 25 to 600 °C at a heating rate of 10 K min<sup>-1</sup>. The specimens were turned to disks of 4 mm diameter and 6 mm high and placed in a hermetic alloy sealed aluminum capsule.

## 2.3. Microstructural characterization

The X-ray diffraction (XRD) measurements were performed using a Philips PW 1800 with Cu-K<sub>α</sub> radiation.

The fracture surfaces of the tensile specimens were examined with a JEOL 6460 LV scanning electron microscope (SEM).

## 2.4. Mechanical tests

Vickers microhardness (HV) tests were performed with a MEKTON hardness tester, at a load of 300 g applied for 30 s. Five measurements were taken at randomly selected points on the middle transverse section of the billet with a diamond pyramidal indenter. Tensile tests were carried out at room temperature using an MTS-810 universal testing machine with a crosshead speed 2 mm min<sup>-1</sup>. In order to ensure the reproducibility of the tensile results, three tests were performed for each condition.

## 3. Results and discussion

The DSC thermograms and the Vickers microhardness measurements, as a function of aging temperature after water quenching of both GC and SC specimens, are plotted in Fig. 2. It is clearly shown that the microhardness of SC alloy is higher than those of the GC alloy. This is a result of the change in microstructure and the densification of an as-cast alloy caused by the applied pressure [6]. The first intense exothermic signal centered at around 70 °C is assigned to the formation of GP zones while the following weak endothermic peaks (around 85 °C) to their dissolution. The wide exothermic peak centered at 170 °C is associated with θ' phase precipitation. These metastable precipitates are responsible for the maximum microhardness values

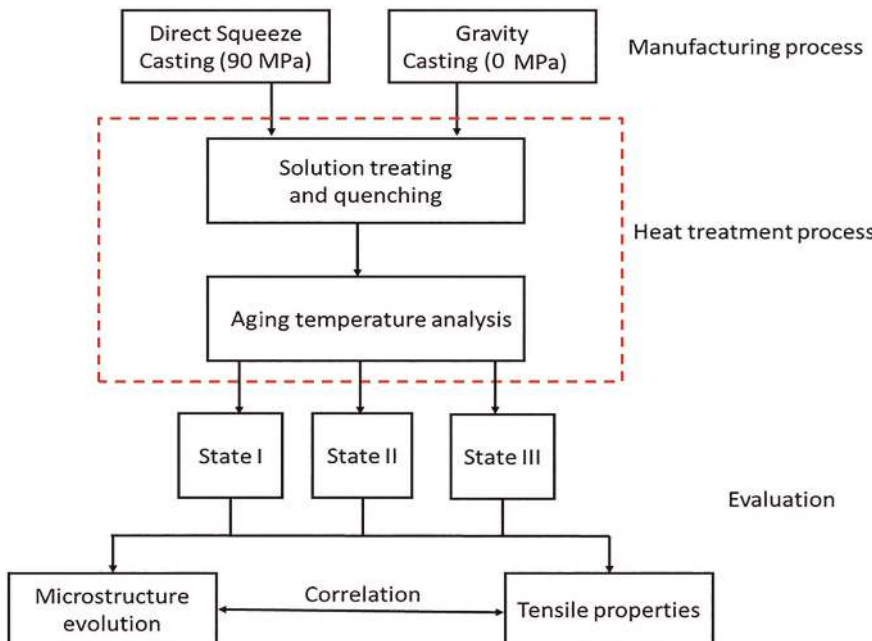


Fig. 1. Experimental set up flowchart.

[18], and this is commonly observed at 180 °C. It was also noticed that the  $\theta''$  peak of the SC (90 MPa) sample is larger than that of the GC (0 MPa), which is consistent with its higher microhardness. However, the wide exothermic peaks at 320 °C are ascribed to the formation of incoherent  $\theta'$  precipitates. Thus, the formation of the latter leads to a substantial decrease in microhardness [18]. Added to that, the intense endothermic peaks at 519 °C for GC and 528 °C for SC specimens are attributed to the melting of the intermetallic compound  $\theta$ -Al<sub>2</sub>Cu [19]. Moreover, the thermal effects associated with  $\theta' \rightarrow \theta$  transformation may not be sufficient to exhibit a separate signal during the DSC scans. As shown in Fig. 2b, this indicates that the peak relative to the melting of  $\theta$  phase is shifted toward higher temperatures with respect to that of GC specimen. This can be attributed

to the increase in eutectic temperature in correlation with the increase in pressure [6].

X-ray diffractograms of the three states of GC and SC samples are illustrated in Fig. 3. The XRD patterns of both cast alloys under 0 MPa (Fig. 3a) and 90 MPa (Fig. 3b) reveal the Bragg reflections of the soluble Al<sub>2</sub>Cu and insoluble Al<sub>12</sub>(Fe,Mn,Cu)<sub>3</sub>Si intermetallic phases. Other residual phases are expected to be dissolved into the matrix by solution treatment. These diffraction results are consistent with those published by Birol [18, 20, 21]. It is also seen that the intensity of the diffraction peaks related to the Al<sub>2</sub>Cu phase tends to broaden with aging temperature, confirming the reported precipitation sequence. This indicates that, during the aging process, the Cu separated out in the form of Al<sub>2</sub>Cu which are predominant precipitates in the alloy.

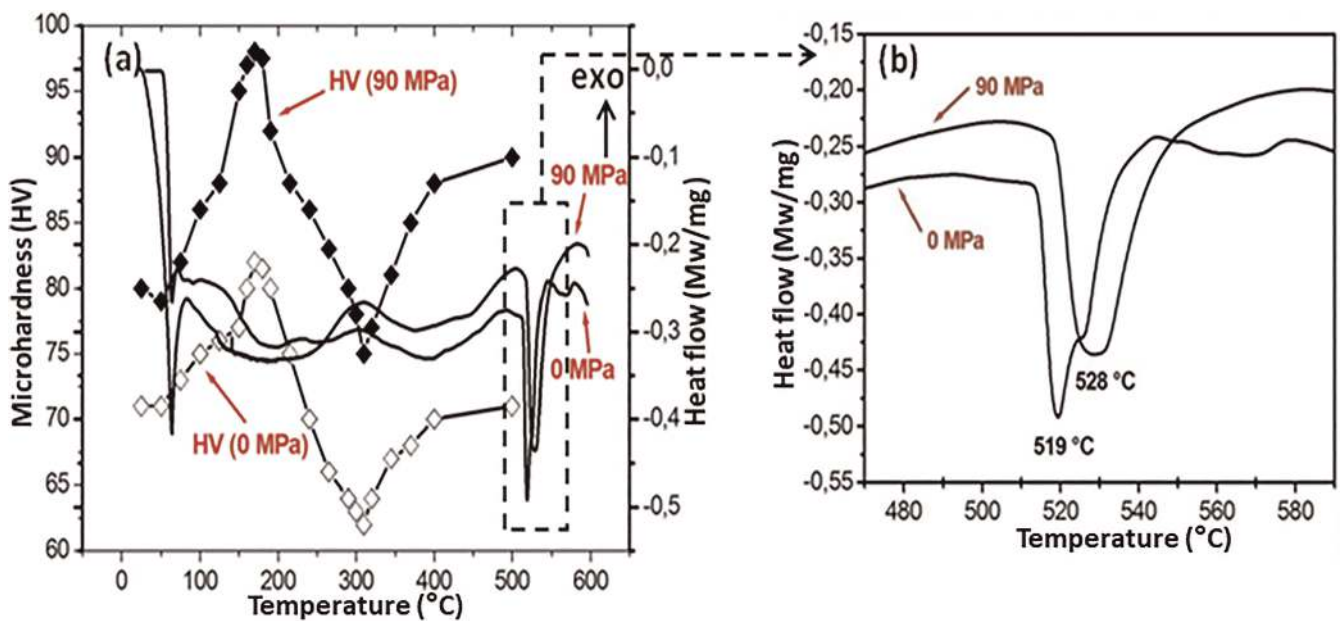


Fig. 2. (a) Microhardness variations and DSC thermograms of GC and SC specimens. (b) Magnification of the DSC curves showing the melting peaks of  $\theta$  phases.

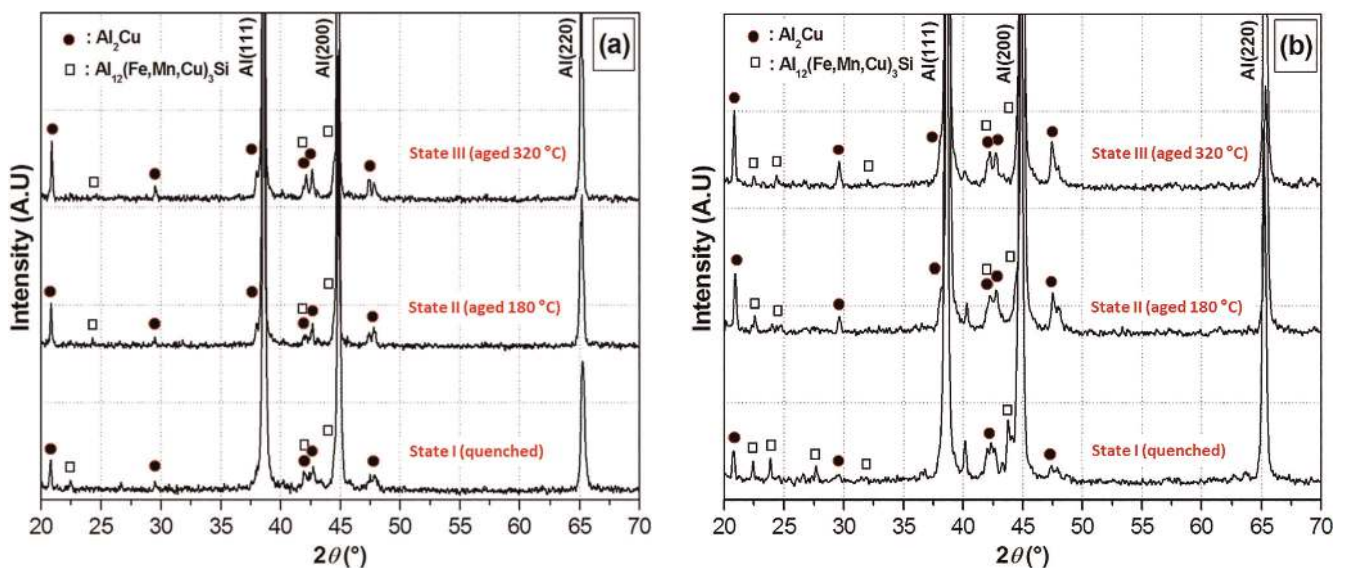


Fig. 3. XRD spectra of (a) GC, and (b) SC samples in the different states.

Figure 4 presents the results of the SEM and EDX (energy dispersive X-ray) analysis of the sample aged at 180 °C prepared by gravity and squeeze casting process, respectively. The SEM-image shows a wide intermetallic precipitation distributed among the grain boundaries, as already observed in the optical micrographs. Also, a lot of shrinkage microporosity is seen in gravity samples (Fig. 4a), while nearly no porosity is observed in squeeze casting samples (Fig. 4b). The predominant phases were identified by EDX (Fig. 4a' and Fig. 4b') analysis once again to be the  $\theta$ -Al<sub>2</sub>Cu intermetallic phases in both GC and SC samples aged at 180 °C.

The tensile properties such as ultimate tensile strength (*UTS*), yield strength (*YS*) and elongation percent (*El%*) of the GC and SC specimens in the different states I (quenched), II (quenched + aged 180 °C) and III (quenched + aged 320 °C) are compiled in Table 2. This shows that the GC specimens have low tensile properties than the SC specimens since the intensity of the applied pressure has a significant influence on the mechanical properties of the 2017 Al alloy [6, 13]. The effect of aging temperature on tensile properties showed that the aging temperature of 180 °C (state II) presents the highest values of *UTS* and *YS* and the lowest value of *El%*. The enhancement of *UTS* and

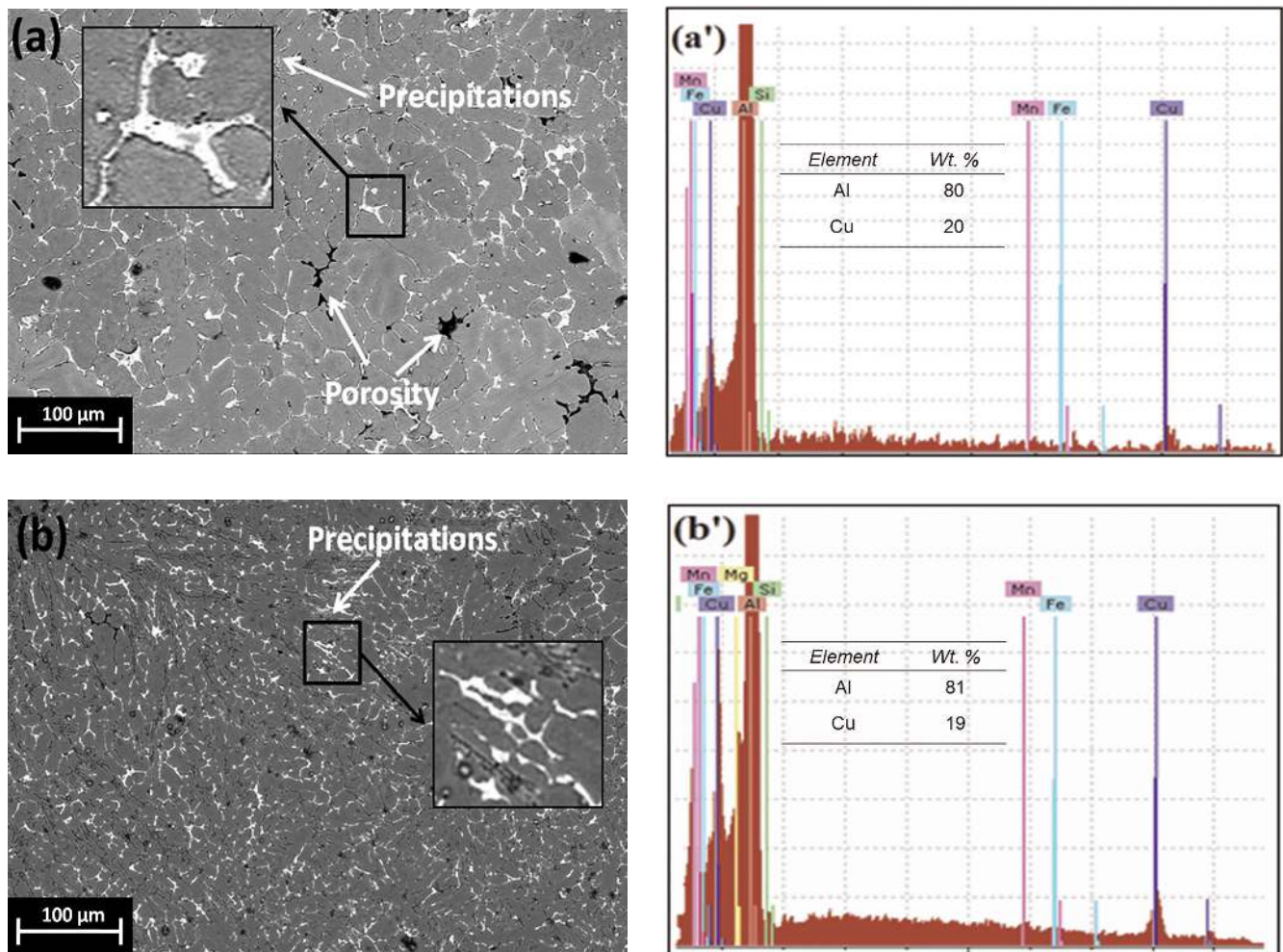


Fig. 4. SEM images and corresponding EDX analysis of: (a, a') gravity, and (b, b') squeeze cast samples each aged at 180 °C.

Table 2. Tensile properties results of the investigated alloy in the different metallurgical states.

Process	Metallurgical state	<i>UTS</i> (MPa)	<i>YS</i> (MPa)	<i>El</i> (%)
GC (0 MPa)	I (quenched)	200	125	1.7
	II (aged 180 °C)	219	175	1.2
	III (aged 320 °C)	175	118	2.5
SC (90 MPa)	I (quenched)	278	199	2.2
	II (aged 180 °C)	298	223	1.85
	III (aged 320 °C)	276	121	3.1

*YS* are likely due to the higher precipitates density of metastable  $\text{Al}_2\text{Cu}$  and insoluble  $\text{Al}_{12}(\text{Fe},\text{Mn},\text{Cu})_3\text{Si}$  precipitates. These precipitates reduce the dislocation movement and thus a higher stress is required for its bowing. It is observed that the best combination of properties, i.e. high *UTS* (298 MPa) and *YS* (223 MPa), is achieved when aging and pressure are at 180 °C and 90 MPa, respectively. In addition as expected, the *El%* varies inversely with the other tensile features. It is thus fair to conclude that the variation of tensile properties with squeeze pressure and heat treatment shows a good synchronized effect with microhardness measurements. This variation is the result of microstructural changes that have been observed previously.

Figure 5 shows typical fracture surfaces of the tensile specimens. On a macroscopic scale, the tensile fracture surface of the GC (0 MPa) specimens is at around 90° angle relative to the load direction for uniaxial tension, which is the characteristic of a brittle fracture surface. However, the SC

(90 MPa) specimens are considered to be ductile and typically fail at approximately 45° with respect to the load direction of the uniaxial tension.

High magnification examination of the fracture surface of the GC specimens shows that the existence of microporosity (see arrows in GC) and the coarse grain size become the principal source of low ductility. This is a typical feature of intergranular fracture paths. Obviously, with no applied pressure, the alloy exhibits shrinkage problems associated with gas porosity due to the low interdendritic fluidity of the molten material [22]. The tensile fracture surface of the SC specimens corresponds to transgranular fracture and reveals that microvoids mostly disappear and that equiaxed dimples occupy a large area. Inclusions and precipitates that initiate the ductile rupture are also observed in the fractography. However, the  $\text{Al}_2\text{Cu}$  intermetallic compounds that inevitably exist at the grain boundaries (see arrows in SC), lead to early fractures by creating notch effects

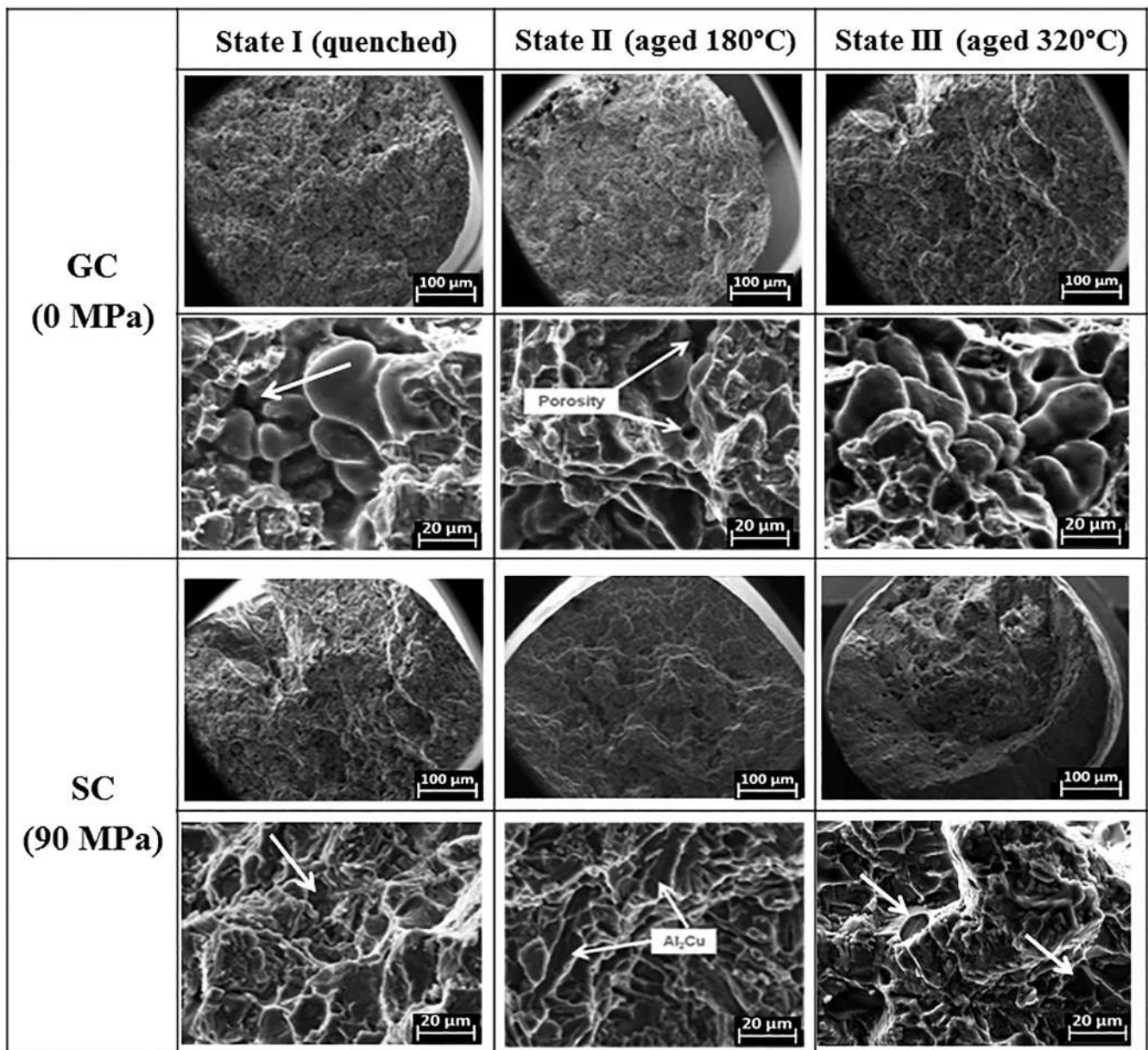


Fig. 5. SEM micrographs of tensile fracture of the selected samples: I, II and III under 0 MPa and 90 MPa.

during the tensile test [23]. It is also revealed that the breakage of intermetallic phases into smaller parts facilitates the dislocation motion. Generally, it can be concluded that the existence of cavities and higher density of precipitates is the principal source of lower ductility.

#### 4. Conclusion

In this study, the effect of squeeze pressure combined with the artificial aging process on the microstructure and the mechanical properties of the cast 2017 A aluminum alloy have been quantified. The conclusions of this work can be summarized as follows:

1. Microhardness evolution of the investigated alloy at various aging temperatures shows that the microhardness increases at first and then decreases as aging temperature increases. The maximum and the minimum values are attained when aging at 180 °C and 320 °C, respectively. In addition, the differential scanning calorimetry (DSC) analysis reveals the transformations of the different phases dissolved in the Al matrix.
2. After aging at 180 °C, the microstructure of both SC and GC alloys was characterized by a high density of metastable precipitates, which corresponds to the maximum value of microhardness.
3. The rise of *UTS*, *YS*, microhardness and the fall of ductility at an aging temperature of 180 °C is more likely due to the precipitation of hard Al<sub>2</sub>Cu phase and the elimination of gas porosity by applied pressure. These results are in good agreement with the microstructural evolution according to the different aging temperatures.
4. The examination via SEM fractography and elongation results of both SC and GC alloys indicates that the fracture mode becomes more ductile at 320 °C.

#### References

- [1] B. Lin, W. Zhang, Z. Lou, D. Zhang, Y. Li: *Mater. Des.* 59 (2014) 10. DOI:10.1016/j.matdes.2014.02.012
- [2] M.T. Abou El khair: *Mater. Lett.* 59 (2005) 894. DOI:10.1016/j.matlet.2004.11.041
- [3] Z. Han, X. Huang, A.A. Luo, A.K. Sachdev, B. Liu: *Scr. Mater.* 66 (2012) 215. DOI:10.1016/j.scriptamat.2011.10.041
- [4] A. Maleki, B. Niroumand, A. Shafyei: *Mater. Sci. Eng. A* 428 (2006) 135. DOI:10.1016/j.msea.2006.04.099
- [5] T.M. Yue: *J. Mater. Process. Technol.* 66 (1997) 179. DOI:10.1016/S0924 0136(96)02516 2
- [6] S.W. Kim, D.Y. Kim, W.G. Kim, K.D. Woo: *Mater. Sci. Eng. A* 304 306 (2001) 721. DOI:10.1016/S0921 5093(00)01594 X
- [7] S.M. Skolianos, G. Kiourtsidis, T. Xatzifotiou: *Mater. Sci. Eng. A* 231 (1997) 17. DOI:10.1016/S0921 5093(97)00067 1
- [8] Z. Ming, Z. Wei wen, Z. Hai dong, Z. Da tong, L. Yuan yuan: *Nonferr. Metal. Soc.* 17 (2007) 496. DOI:10.1016/S1003 6326(07)60122 8
- [9] J. da Costa Teixeira, D.G. Cram, L. Bourgeois, T.J. Bastow, A.J. Hill, C.R. Hutchinson: *Acta Mater.* 56 (2008) 6109. DOI:10.1016/j.actamat.2008.08.023

- [10] K. Saï, L. Taleb, G. Cailletaud: *Comput. Mater. Sci.* 65 (2012) 48. DOI:10.1016/j.commat.2012.06.035
- [11] G. Giuliano: *Manuf. Letters*. 10 (2016) 10. DOI:10.1016/j.mfglet.2016.08.003
- [12] N. Souissi, S. Souissi, J. Lecompte, M.B. Amar, C. Bradai, F. Halouani: *Int. J. Adv. Manuf. Technol.* 78 (2015) 2069. DOI:10.1007/s00170 015 6792 0
- [13] N. Souissi, S. Souissi, C.L. Niniven, M.B. Amar, C. Bradai, F. Halouani: *Metals* 4 (2014) 141. DOI:10.3390/met4020141
- [14] N. Souissi, S. Souissi, C.L. Niniven, M.B. Amar, C. Bradai, F. Halouani: *Int. J. Mater. Eng. Innovation* 6 (2015) 59. DOI:10.1504/IJMATEI.2015.069801
- [15] M.B. Amar, S. Souissi, N. Souissi, C. Bradai: *Int. J. Microstruct. Mater. Prop.* 7 (2012) 491. DOI:10.1504/IJMMP.2012.051229
- [16] C. Vargel: *The most common wrought aluminum alloys. In corrosion of aluminium*; Elsevier, Amsterdam, The Netherlands (2004) 65 66. DOI:10.1016/B978 008044495 6/50009 4
- [17] *Metallic materials and elements for aerospace vehicle structures. Military: Handbook 5H.*, US Department of Defense, USA (1998).
- [18] Y. Birol: *Mater. Sci. Eng. A* 528 (2011) 5636. DOI:10.1016/j.msea.2011.03.101
- [19] B. Zlaticanin, B. Radonjic, M. Filipovic: *Mater. Sci. Forum* 453 454 (2004) 193. DOI:10.4028/www.scientific.net/MSF.453 454.193
- [20] Y. Birol: *J. Mater. Proc. Technol.* 211 (2011) 1749. DOI:10.1016/j.jmatprotec.2011.05.016
- [21] Y. Birol: *Mater. Chem. Phys.* 131 (2012) 694. DOI:10.1016/j.matchemphys.2011.10.036
- [22] E. Hajjari, M. Divandari: *Mater. Des.* 29 (2008) 1685. DOI:10.1016/j.matdes.2008.04.012
- [23] W. Dai, S. Wu, S. Lü, C. Lin: *Mater. Sci. Eng. A* 538 (2012) 320. DOI:10.1016/j.msea.2012.01.051

(Received December 24, 2018; accepted March 23, 2019; online since July 10, 2019)

#### Correspondence address

Najib Souissi  
 Ravago Middle East Company  
 Industrial city 2 Cross Road 308 & 315  
 PO BOX 10311, Jubail 35748  
 Saudi Arabia.  
 Tel.: +966509279529  
 +21621134957  
 E mail: souissi.najib@gmail.com  
 souissi.nejib@yahoo.fr